

Article

Microbial Biosynthesis of Chrysazin Derivatives in Recombinant *Escherichia coli* and Their Biological Activities

Purna Bahadur Poudel ^{1,†}, Dipesh Dhakal ^{1,†}, Rubin Thapa Magar ¹ and Jae Kyung Sohng ^{1,2,*}

¹ Institute of Biomolecule Reconstruction (iBR), Department of Life Science and Biochemical Engineering, Sun Moon University, 70 Sun Moon-ro 221, Tangjeong-myeon, Asan-si 31460, Chungnam, Korea

² Department of Biotechnology and Pharmaceutical Engineering, Sun Moon University, 70 Sun Moon-ro 221, Tangjeong-myeon, Asan-si 31460, Chungnam, Korea

* Correspondence: sohng@sunmoon.ac.kr; Tel.: +82-(41)-530-2246; Fax: +82-(41)-530-8229

† These authors contributed equally to this work.

Abstract: Anthraquinone and its derivatives show remarkable biological properties such as anticancer, antibacterial, antifungal, and antiviral activities. Hence, anthraquinones derivatives have been of prime interest in drug development. This study developed a recombinant *Escherichia coli* strain to modify chrysazin to chrysazin-8-O- α -L-rhamnoside (CR) and chrysazin-8-O- α -L-2'-O-methylrhamnoside (CRM) using rhamnosyl transferase and sugar-O-methyltransferase. Biosynthesized CR and CRM were structurally characterized using HPLC, high-resolution mass spectrometry, and various nuclear magnetic resonance analyses. Antimicrobial effects of chrysazin, CR, and CRM against 18 superbugs, including 14 Gram-positive and 4 Gram-negative pathogens, were investigated. CR and CRM exhibited antimicrobial activities against nine pathogens, including methicillin-resistant *Staphylococcus aureus* (MRSA) and methicillin-sensitive *Staphylococcus aureus* (MSSA) in a disk diffusion assay at a concentration of 40 μ g per disk. There were MIC and MBC values of 7.81–31.25 μ g/mL for CR and CRM against methicillin-sensitive *S. aureus* CCARM 0205 (MSSA) for which the parent chrysazin is more than >1000 μ g/mL. Furthermore, the anti-proliferative properties of chrysazin, CR, and CRM were assayed using AGS, Huh7, HL60, and HaCaT cell lines. CR and CRM showed higher antibacterial and anticancer properties than chrysazin.

Keywords: rhamnosyltransferase; O-methyltransferase; chrysazin; biological properties



Citation: Poudel, P.B.; Dhakal, D.; Magar, R.T.; Sohng, J.K. Microbial Biosynthesis of Chrysazin Derivatives in Recombinant *Escherichia coli* and Their Biological Activities. *Molecules* **2022**, *27*, 5554. <https://doi.org/10.3390/molecules27175554>

Academic Editor: Changsheng Zhang

Received: 22 July 2022

Accepted: 24 August 2022

Published: 29 August 2022

Publisher's Note: MDPI stays neutral with regard to jurisdictional claims in published maps and institutional affiliations.



Copyright: © 2022 by the authors. Licensee MDPI, Basel, Switzerland. This article is an open access article distributed under the terms and conditions of the Creative Commons Attribution (CC BY) license (<https://creativecommons.org/licenses/by/4.0/>).

1. Introduction

Quinones are naturally occurring organic compounds found in higher plants, fungi, bacteria, and animals. They have a lot of structural varieties. Since they are found in different colors in nature, they are considered pigments [1]. Anthraquinones are the largest group of quinones, with various biological properties such as antioxidant [2], antifungal [3], antiviral [4], anti-diabetic [5], anti-inflammatory [6], and laxative [7] effects. They are also used as natural dyes in industries [8]. Several anthraquinones are widely used in the treatment of cancer [9–11]. They show cytotoxic activities through interaction with DNA, preferentially at cytosine/guanine-rich sites [12].

Synthesis of anthraquinone derivatives is of great interest recently. There are various methods for the synthesis of anthraquinones derivatives, including intramolecular condensation of aryl and o-aryloxybenzoic acid using fuming sulfuric acid, benzoyl chloride, concentrated sulfuric acid, benzoyl chloride, zinc chloride, and POCl₃/P₂O₃Cl₄ [13]. The chemical synthesis of anthraquinones derivatives is an expensive and difficult process [14].

Modification of anthraquinones can be performed by glycosylation, methylation, sulfation, prenylation, and so on. Glycosylation is an important process for increasing the solubility of hydrophobic compounds, improving stability, reducing toxicity, and modifying biological activities [15,16]. Methylation can alter the solubility, deactivate the reactive

hydroxyl group, increase the metabolic stability, increase membrane transport, and increase pharmaceutical properties [17–19].

Methyltransferases are important enzymes in the modification of different substrate. However, methylation of sugar is very rare [20,21]. Generally, transfer of the sugar group is catalyzed by glycosyltransferases (GTs) with activated NDP-sugars as sugar donors. Methylation reactions are catalyzed by *O*-methyltransferase (OMT) that catalyzes the transfer of the methyl group of *S*-adenosyl-L-methionine (SAM) to hydroxyl groups [15,22,23].

Chryszin (Dantrol; 1,8 dihydroxyanthraquinone) has been used as a medicine since ancient times. It can be found naturally. It is isolated from the root and rhizome of *Rheum palmatum L.* (Polygonaceae) [24]. It has a wide range of activities, such as antitumor activity, confirmed by different experiments [24,25].

This study is based on the utilization of indigenous *E. coli* sugar (thymidine diphosphate (TDP)-rhamnose) as a sugar donor, which will be used as a glycosyltransferase to conjugate to chryszin and SAM as an *O*-methyltransferase to conjugate chryszin rhamnoside. For the production of chryszin derivatives, anthraquinone rhamnosyltransferase (7665) [26] from *Saccharothrix espanaensis* and *O*-methyltransferase (ThnM1) [27] from *No-cardia sp.* CS682 were cloned and heterologously expressed in *E. coli*. The recombinant strain *E. coli* was utilized for the production of chryszin-8-*O*- α -L-rhamnoside (CR) and chryszin-8-*O*- α -L-2'-*O*-methylrhamnoside (CRM) from the substrate chryszin (Figure 1). Anticancer and antibacterial activities of CR and CRM were assessed and results were compared to those of chryszin.

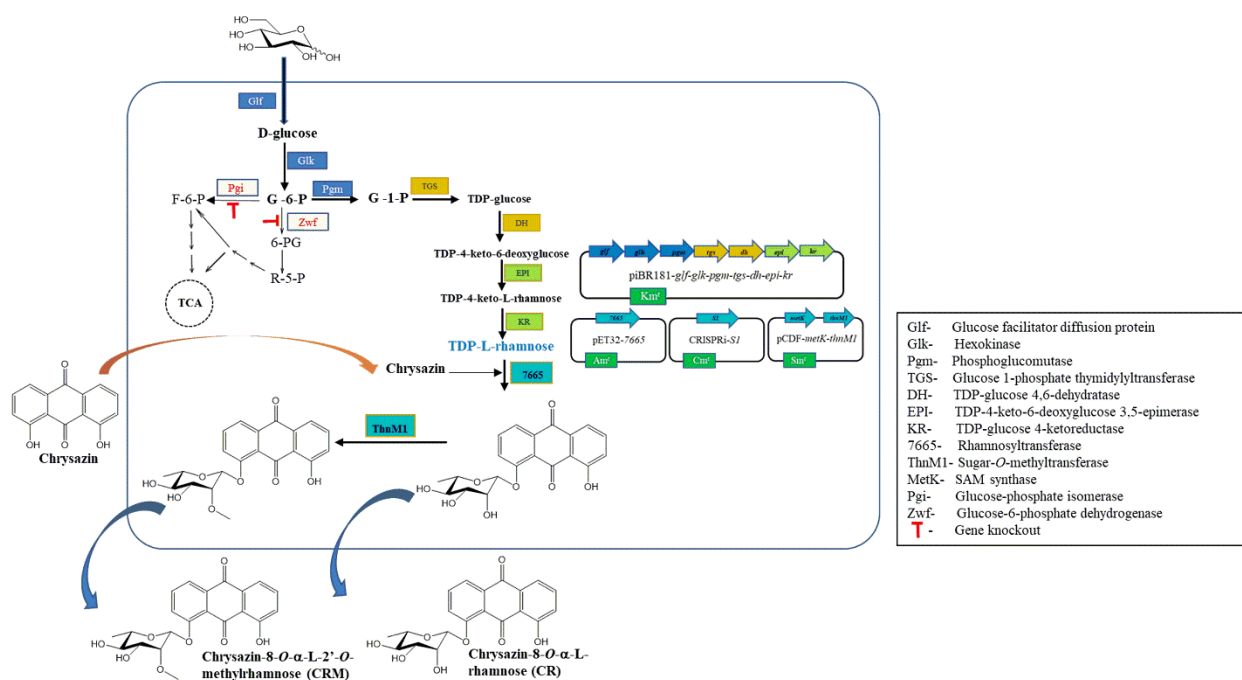


Figure 1. A scheme showing the pathway of utilizing recombinant *Escherichia coli* BL21(DE3) for the biosynthesis of chryszin-8-*O*- α -L-rhamnoside (CR) and chryszin-8-*O*- α -L-2'-*O*-methylrhamnoside (CRM) from chryszin. Chromosomal *pgi* (glucose-phosphate isomerase) and *zwf* (glucose-6-phosphate dehydrogenase) genes were knocked-out. Chromosomal *glk* (hexokinase), *pgm* (phosphoglucumutase), *tgs* (glucose 1-phosphate thymidyltransferase), *dhl* (TDP-glucose 4,6-dehydratase), *epi* (TDP-4-keto-6-deoxyglucose 3,5-epimerase), and *kr* (TDP-glucose 4-ketoreductase) genes were overexpressed by cloning into pIBR181. 7665 (rhamnosyl transferase) was overexpressed by cloning into pET32a (+), and *metK* (SAM synthase) and *thnM1* (sugar-*O*-methyltransferase) were overexpressed by cloning into pCDF-Duet.

2. Materials and Methods

2.1. General Procedures

Chrysazin/Dantron was purchased from Tokyo Chemical Industry (Tokyo, Japan). HPLC-grade acetonitrile and water were purchased from Mallinckrodt Baker (Phillipsburg, NJ, USA). All other chemicals used were of high analytical grade and commercially available. Isopropyl- β -D-1-thiogalactoside (IPTG) was purchased from GeneChem Inc. (Daejeon, Korea). SAM was purchased from Sigma-Aldrich (St. Louis, MO, USA). *Escherichia coli* BL21 (DE3) (Stratagene, La Jolla, CA, USA) was used as an expression and biotransformation host. Luria–Bertani (LB) broth medium and agar plates with appropriate antibiotics (ampicillin, kanamycin, chloramphenicol, and streptomycin, each at 50 μ g/mL) were used for culture preparation, colony selection, and biotransformation. Pathogenic strains such as *Staphylococcus aureus* CCARM 3640 (MRSA), *S. aureus* CCARM 3089 (MRSA), *S. aureus* CCARM 33591 (MRSA), *S. aureus* CCARM 0205 (MSSA), *S. aureus* CCARM 0204 (MSSA), *S. aureus* CCARM 0027 (MSSA), *S. aureus* CCARM 3090 (MRSA), *S. aureus* CCARM 3634 (MRSA), *S. aureus* CCARM 3635 (MRSA), *Bacillus subtilis* ATCC 6633, *Enterococcus faecalis* 19433, *Enterococcus faecalis* 19434, *Kocuria rhizophilla* NBRC 12708, *Micrococcus luteus*, *Escherichia coli* ATCC 25922, *Proteus hauseri* NBRC 3851, *Klebsiella pneumonia* ATCC10031, and *Salmonella enterica* ATCC 14,028 were obtained from Professor Seung-Young Kim (Sun Moon University, Korea) [28].

2.2. Generation of Recombinant Strains

For the production of rhamnosylated and methoxy-rhamnosylated derivatives of chrysazin using engineered *E. coli*, anthraquinone rhamnosyltransferase (7665) [29] from *S. espanaensis* and rhamnose methyltransferase (ThnM1) [27] from *Nocardia* sp. CS682 were taken to prepare *E. coli* S2 [30]. *E. coli* S2 was generated by transforming pET32a \pm 7665(Am) CRISPRi-S1(Cm^r) and pCDFDuet-metK-thnM1(Sm) into an *E. coli* strain harboring the rhamnose cassette piBR181-tgs.dh.ep.kr.pgm2.glf.glk (Km) [31]. Recombinant plasmids were confirmed by restriction endonuclease activity as well as by growing in a combined four-antibiotic LB agar plate and LB broth medium.

2.3. Culture Preparation and Whole-Cell Biotransformation

A seed culture of *E. coli* S2 was cultured in a 5 mL LB medium supplemented with ampicillin, kanamycin, chloramphenicol, and streptomycin (each at 50 μ g/mL) and incubated at 37 °C for 3 h. From the 5 mL seed culture, 500 μ L was transferred into a flask containing 50 mL LB broth with respective antibiotics and cultured at 37 °C for around 4 h until the optical density of cells at 600 nm (OD₆₀₀) reached 0.6–0.8. This culture had added to it 0.5 mM isopropyl β -D-1-thiogalactopyranoside (IPTG) to induce protein expression, followed by incubation at 20 °C for 20 h. To determine optimal substrate concentration, glucose concentration, and time, different concentrations (1, 2, 4, 6, 8, 10 mM) of chrysazin and different concentrations (2%, 5%, 10%, 12%, and 15%) of sterile glucose solution were fed into the cell culture after induction. After 20 h of adding IPTG, chrysazin dissolved in dimethyl sulfoxide (DMSO) at a final concentration of 400 μ M was added along with 10% glucose. Samples (3 mL of culture broths) were withdrawn at 6, 12, 24, 36, 48, and 60 h for product analysis. After 48 h, compounds were extracted using a double volume of ethyl acetate (2:1, v/v) and a Soxhlet extractor. The Soxhlet extractor was kept still to separate the mixture for 4–6 h at room temperature after shaking. Ethyl acetate was removed under reduced pressure and dissolved in methanol. This sample was further analyzed by HPLC and mass spectrometry. To collect a sample to characterize structurally, the biotransformation experiment was performed using a fermenter (3 L of culture). The pure fraction of the compound was collected via preparatory-high-pressure liquid chromatography (prep-HPLC).

2.4. Analytical Procedures

From the extracted compound, a 20 μ L volume was injected and directly analyzed by reverse-phase high-performance liquid-chromatography photo-diode array (HPLC-PDA) using a Thermo Scientific Dionex Ultimate 3000 ultrahigh-performance Liquid chromatography (UHPLC) system with a reverse-phase C₁₈ column (Mightysil RP-18 GP (4.6 mm \times 250 mm, 5 μ m particle size) (Kanto Chemical, Tokyo, Japan)). The binary mobile phase was composed of solvent A (HPLC-grade water + 0.1% trifluoroacetic acid) and solvent B (100% acetonitrile, ACN). The total flow rate was maintained at 1 mL/min for the 30 min program. The ACN concentration began with 10%. A linear gradient from 10 to 50% for 10 min, 50–90% for 23 min, and 90–10% for 30 min was then used. The HR-QTOF ESI/MS was performed in positive ion mode using an Acquity mass spectrometer (Waters, Milford, MA, USA), which was coupled with a Synapt G2-S system (Waters). Purification of compounds was performed using a prep-HPLC instrument equipped with a YMC-Pack ODS-AQ C₁₈ column, (150 \times 20 mm I.D., mean particle size: 10 μ m) (YMC America, Inc., Devens, MA, USA) and a connected UV detector (420 nm). Here, a 40 min binary program with implementation of 20% (0–5 min), 50% (5–10 min), 70% (10–20 min), 90% (20–25 min), 20% (25–30 min), and 10% (30–35 min) ACN at a flow rate of 10 mL/min was used. Purified products were pooled, dried, and lyophilized to remove water or moisture. Furthermore, the fully dried pure compound was dissolved in DMSO-*d*₆ and subjected to a 700 MHz NMR spectrometer equipped with TCI CryoProbe (5 mm).

One-dimensional NMRs (¹H NMR and ¹³C NMR) and two-dimensional NMRs (heteronuclear multiple quantum coherence (HMQC), rotating frame Overhauser enhancement spectroscopy (ROESY), and heteronuclear multiple bonded connectivity (HMBC)) were used as needed to elucidate the structure of the compound.

2.5. Anticancer Activities of Chrysozin, CR, and CRM

Three cancer cell lines (i.e., human liver cancer cell line (Huh7), human gastric cancer cell line (AGS), and human leukemia cell line (HL60) and normal cell line (human keratinocyte cell line (HaCaT) were purchased from Korean Cell Line Bank (Seoul, Korea). Huh7 cells were cultured in Dulbecco's modified Eagle's medium (DMEM) (Corning Cellgro Manassas, VA, USA) and AGS cells were cultured in Roswell Park Memorial Institute 1640 medium (RPMI1640) (Corning Cellgro, Manassas, VA, USA) supplemented with 10% fetal bovine serum (FBS) (Grand Island, NY, USA) and 1% penicillin-streptomycin-amphotericin B (Walkersville, MD, USA). Human leukemia HL60 cells were cultured in RPMI1640 supplemented with 10% FBS, 1% penicillin-streptomycin-amphotericin B, and L-glutamine (2 mm) (Grand Island, NY, USA). HaCaT cell lines were grown in DMEM supplemented with 10% FBS, 100 μ g/mL streptomycin, and 100 μ g/mL benzylpenicillin. All cells were maintained at 37 °C in a humidified 5% CO₂ incubator. For cell growth assay, cells were seeded at 3 \times 10² cells/well into white 96-well culture plates (SPL Life Sciences, Pochon, Korea), incubated at 37 °C in a humidified 5% CO₂ overnight, and then treated with each compound after serial dilution (200 μ M, 100 μ M, 50 μ M, 25 μ M, 12.5 μ M, 6.25 μ M, 3.16 μ M, 1.56 μ M, 0.78 μ M) for 72 h. After that, 20 μ L substrate solution (Promega) was added to each well. The plate was shaken for 5 min and kept in the dark for 10 min. Luminescence was measured using a multimode plate reader (BioTek, Inc., Winooski, VT, USA). IC₅₀ values were analyzed using GraphPad Prism 5 (GraphPad Software, La Jolla, CA, USA).

2.6. Antimicrobial Activities of Chrysozin, CR, and CRM

2.6.1. Disk Diffusion Assay

Fourteen Gram-positive bacteria (*Staphylococcus aureus* CCARM 3640 (MRSA), *S. aureus* CCARM 3089 (MRSA), *S. aureus* CCARM 33591 (MRSA), *S. aureus* CCARM 0205 (MSSA), *S. aureus* CCARM 0204 (MSSA), *S. aureus* CCARM 0027 (MSSA), *S. aureus* CCARM 3090 (MRSA), *S. aureus* CCARM 3634 (MRSA), *S. aureus* CCARM 3635 (MRSA), *Bacillus subtilis* ATCC 6633, *Enterococcus faecalis* 19433, *Enterococcus faecalis* 19434, *Kocuria rhizophilla* NBRC

12708, and *Micrococcus luteus*) and four Gram-negative bacteria (*Escherichia coli* ATCC 25922, *Proteus hauseri* NBRC 3851, *Klebsiella pneumonia* ATCC10031, and *Salmonella enterica* ATCC 14028) were used to test antibacterial activities of chrysazin and its derivatives. The paper disk diffusion assay on the Mueller–Hinton agar (MHA) plate was carried out according to Clinical Laboratory Standard Institute (CLSI) guidelines and the Kirby–Bauer method [32,33]. Inocula containing 10^8 colony forming units (CFU)/mL were spread onto MHA plates. Then, 40 μg /disk compounds were placed on the surface of inoculated agar plates using sterile paper disks of 6 mm (Advantec, Toyo Roshi Kaisha, Ltd., Japan). Samples were then incubated at 37 °C for 18–20 h. The zone of inhibition diameter was measured in millimeters for each pathogen. Dimethyl sulfoxide (DMSO) was used as a control for the zone of inhibition as all compounds were dissolved in DMSO.

2.6.2. Measurements of MIC and MBC of Chrysazin Derivatives

The following nine strains were used in the minimum inhibitory concentration (MIC) and minimum bactericidal concentration (MBC) tests: *Staphylococcus aureus* CCARM 3640 (MRSA), *S. aureus* CCARM 3089 (MRSA), *S. aureus* CCARM 33591 (MRSA), *S. aureus* CCARM 0205 (MSSA), *S. aureus* CCARM 0204 (MSSA), *S. aureus* CCARM 0027 (MSSA), *S. aureus* CCARM 3090 (MRSA), *S. aureus* CCARM 3634 (MRSA), and *S. aureus* CCARM 3635 (MRSA). They were grown in Mueller–Hinton Broth (MHB) (Difco, Baltimore, MD, USA). The broth dilution method was used to determine MIC [34]. The MHB and sample were dispensed in a 96-well plate and serially diluted. The strain was inoculated into each well and cultured for 16–20 h at 37 °C. Each strain's suspension was adjusted to 0.5 McFarland standard (1×10^8 CFU/mL) and then diluted to 2.5×10^6 CFU/mL in MHB. After knowing the MIC, the MBC test was performed on a fresh MHB medium by inoculating cultured samples containing MIC compounds and experimental strains.

3. Results and Discussion

3.1. Biosynthesis of CR and CRM

The recombinant strain of *E. coli* strain S2 was generated by engineering *E. coli* BL21 (DE3), which contained a sugar transfer cassette and a sugar methylation cassette. It was cultured and prepared for biotransformation as mentioned in Section 2.2. For optimal production, different concentrations (1, 2, 4, 6, 8, and 10 mm) of chrysazin and different concentrations (2%, 5%, 10%, 12%, and 15%) of glucose were tested with different time intervals (6, 12, 24, 36, 48, and 60 h). It was observed that 400 μM , 10% glucose, and 48 h were suitable conditions (Figure S1). The biotransformation system was induced with 0.5 mM of IPTG. After 20 h, 400 μM of chrysazin and 10% glucose were supplied into cell cultures. The extract from engineered *E. coli* strain S2 was analyzed by HPLC. The HPLC chromatogram of chrysazin was obtained with its standard retention time (tR) of 21.3 min. Two new peaks of CR and CRM were obtained at tR of 14.9 min and 16.3 min, respectively, with UV absorbance at 420 nm (Figure 2). The reaction mixture was further analyzed by high-resolution quadrupole time-of-flight electrospray ionization mass spectrometry (HR-QTOF ESI/MS). The product mass fragment of CR $[\text{M} + \text{H}]^+ m/z = 387.1047$ was matched to the calculated mass of CR $[\text{M} + \text{H}]^+ m/z = 387.1074$. Similarly, the product mass fragment of CRM $[\text{M} + \text{Na}]^+ m/z = 423.1057$ was matched to the calculated mass $[\text{M} + \text{Na}]^+ m/z = 423.1056$ in the positive ion mode (Figure 3), which resembled the rhamnosylated and rhamnose-methylated derivatives of chrysazin.

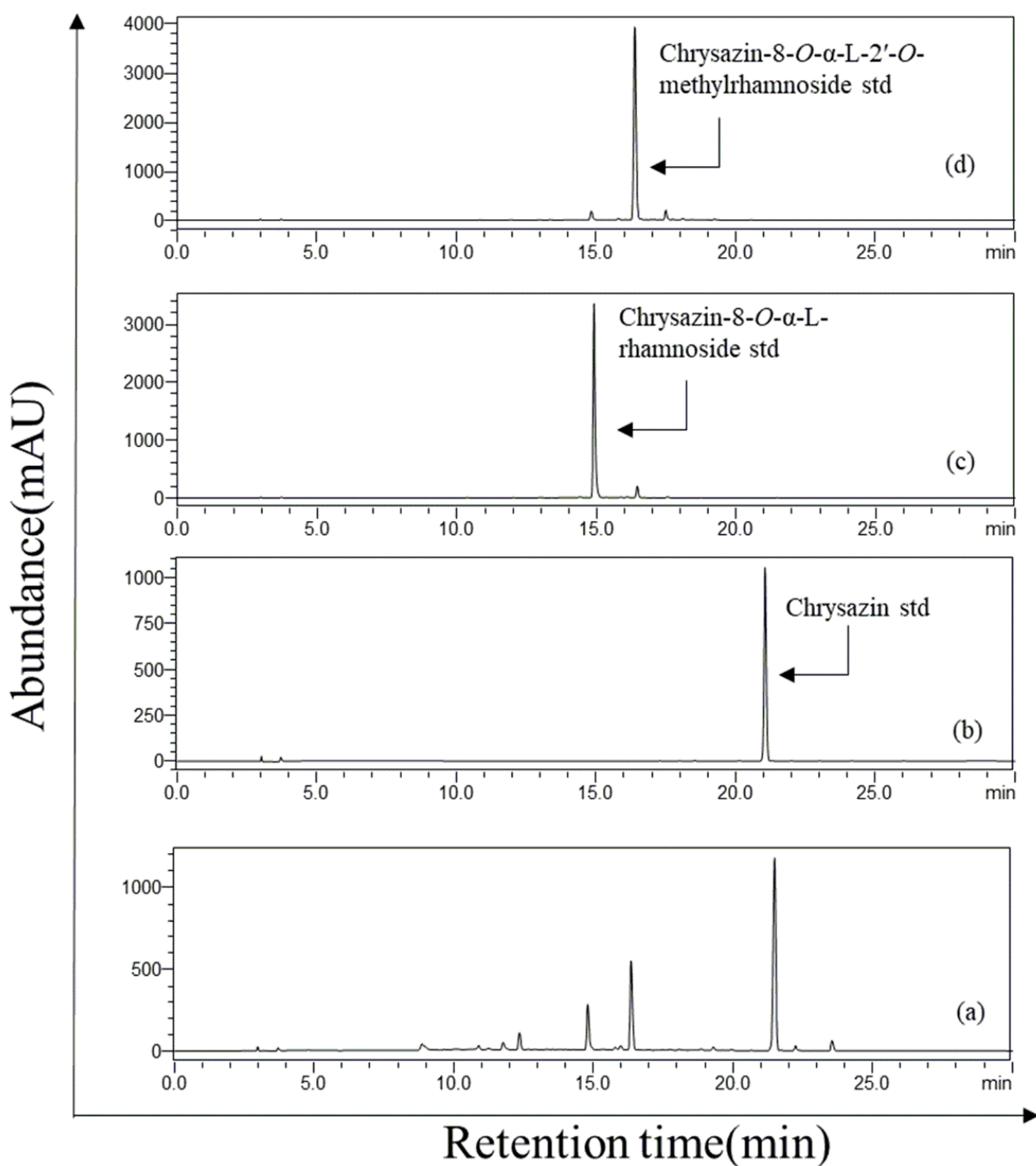


Figure 2. Whole-cell biotransformation of chrysin to chrysin-8-O- α -L-rhamnoside and chrysin-8-O- α -L-2'-O-methylrhamnoside using engineered *E. coli* S2 overexpressing anthraquinone glycosyltransferase, sugar-MT (ThnM1), TDP-rhamnose sugar biosynthetic pathway overexpressing plasmid, and SAM synthase overexpressing plasmid. HPLC-PDA chromatogram analyses of (a) biotransformation reaction sample compared to (b) chrysin standard, (c) chrysin-8-O- α -L-rhamnoside standard, (d) chrysin-8-O- α -L-2'-O-methylrhamnoside.

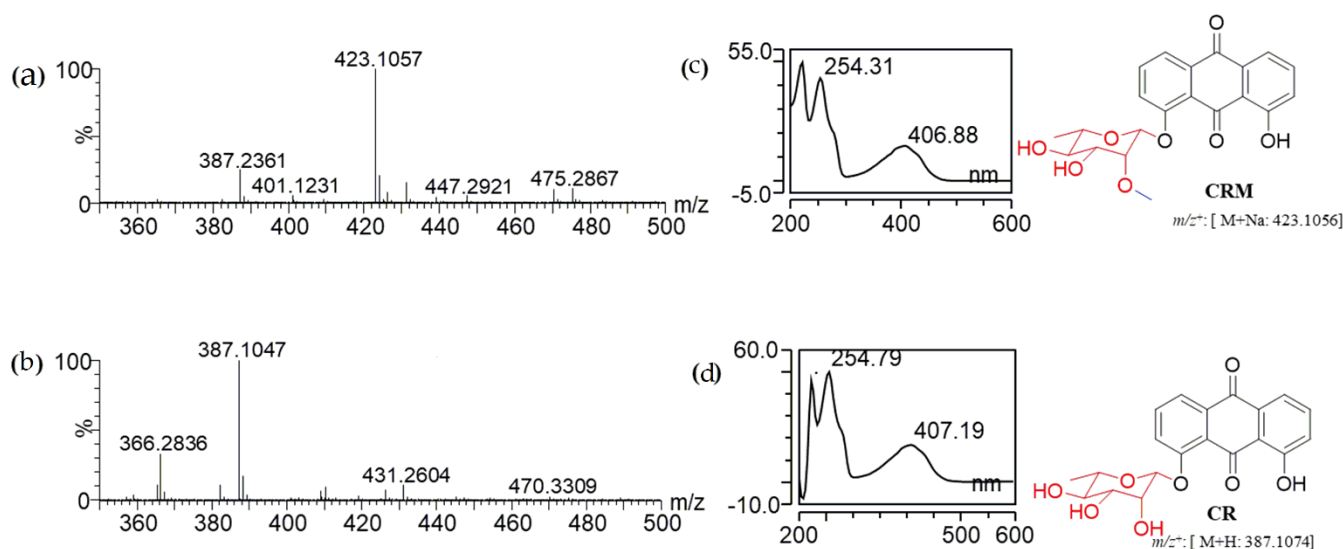


Figure 3. HR-QTOF ESI/MS chromatogram of (a) chrysazin-8-*O*- α -L-2'-*O*-methylrhamnoside; (b) chrysazin-8-*O*- α -L-rhamnoside; (c) UV/VIS of CRM, (d) UV/VIS of CR.

3.2. Purification and Structural Elucidation of the Metabolite

Biotransformation was carried out through fermentation to collect CR and CRM for structure identification and further biological activity tests. The biotransformation reaction mixture was extracted with a double volume of ethyl acetate. The crude extract was subjected to preparatory-high-pressure liquid chromatography (prep-HPLC) for purification. After several rounds of prep-HPLC, purified compounds were obtained. The purified product was dried by lyophilization, dissolved in 400 μ L of deuterated dimethyl sulfoxide, and analyzed by nuclear magnetic resonance (NMR) spectroscopy (700 MHz) including 1D NMR (^1H -NMR and ^{13}C -NMR) and 2D NMR (HMBC, HSQC, COSY, and ROESY), as shown in Figures S2–S4, and Table 1 for structural elucidation.

The ^1H -NMR of chrysin, CR, and CRM showed multiple peaks between 1.0 ppm and 13.0 ppm. In the case of CR, the rhamnose group was attached to the 8-OH group of chrysin. The anomeric proton (1'-H) was consistent with δ 5.67 (d, $J = 1.1$ Hz, 1H), in which the anomeric proton coupling constant ($J = 1.1$ Hz) confirmed that the conjugation of rhamnose moiety had an α -configuration. In addition, with ^{13}C -NMR of CR, the anomeric carbon peak appeared at δ 99.08 ppm, with other peaks appearing between 70 and 80 ppm along with a CH_3 peak at 18.35 ppm. In the case of CRM, there was a methylation in the 2'-OH group of rhamnose in CR, where the OCH_3 spectrum was visible in both ^1H and ^{13}C NMR at 3.5 ppm and 59.44 ppm, respectively. Furthermore, to confirm the sugar and sugar-*O*-methylation conjugation, two-dimensional (2D)-NMR analyses such as ^1H - ^{13}C HSQC, ^1H - ^{13}C HMBC, ^1H - ^1H COSY, and ^1H - ^1H ROESY experiments were performed. Similarly, in CR, HSQC showed a cross peak illustrating a correlation between the anomeric C-1' proton (δ 5.67 ppm) and the anomeric carbon (δ 99.00 ppm). Moreover, the C-8 signal appearing at δ 157.18 ppm showed a direct correlation with the observed anomeric proton at δ 5.67 ppm in HMBC (Figure S3). In the case of CRM, HSQC showed a cross peak illustrating a correlation between the C-2' protons (δ 3.71 ppm) and the carbon (δ 80.61 ppm), and HMBC showed a cross peak depicting the correlations between C-2' (δ 80.62 ppm) and the protons of the methoxy group (δ 3.50 ppm) (Figure S4). Results shown above reveal that the glycosylated derivative of chrysin (i.e., the chrysin-8-*O*- α -L-rhamnoside) and methylated derivative of CR (i.e., chrysin-8-*O*- α -L-2'-*O*-methylrhamnoside) produced by *E. coli* S2 whole-cell biotransformation were new compounds.

Table 1. Comparison of ^1H - and ^{13}C -NMR chemical shifts of chrysozin, chrysozin-8- O - α -L-rhamnoside (CR), and chrysozin-8- O - α -L-2'- O -methylrhamnoside (CRM) measured in DMSO- d_6 solvent.

Position	^1H -NMR (700 MHz, DMSO- d_6)			^{13}C -NMR (176 MHz, DMSO- d_6)		
	Chrysozin	CR	CRM	Chrysozin	CR	CRM
1				161.35	161.94	161.94
2	7.37 (dd, $J = 8.4$ Hz, 1H)	7.64 (dd, $J = 7.5$ Hz, 1H)	7.32 (d, $J = 8.5$ Hz, 1H)	124.44	118.81	124.67
3	7.8 (m, 1H)	7.74 (dd, $J = 7.9$ Hz, 1H)	7.71 (m, 1H)	137.48	136.80	123.72
4	7.70 (dd, $J = 7.5$ Hz, 1H)	7.35 (dd, $J = 8.3$ Hz, 1H)	7.60 (d, $J = 7.3$ Hz, 1H)	119.33	124.69	118.80
4a				133.29	132.87	132.79
5	7.70 (dd, $J = 7.5$ Hz, 1H)	7.85 (d, $J = 2.3$ Hz, 1H)	7.84 (m, 1H)	119.33	136.42	136.34
6	7.8 (m, 1H)	7.85 (s, 1H)	7.70 (d, $J = 13.3$ Hz, 1H)	137.48	121.02	136.78
7	7.37 (dd, $J = 8.4$ Hz, 1H)	7.69 (ddd, $J = 9.6$ Hz, 1H)	7.84 (m, 1H)	124.44	123.31	121.21
8	7.99 (dd, $J = 5.79$, 3.31 Hz, 1H)			161.35	157.27	157.19
8a				115.93	121.39	121.49
9				192.02	188.63	188.57
9a				115.93	117.21	117.15
10				181.37	182.35	188.90
10a				133.29	135.47	135.39
11	11.90 (s, 1H)	12.98 (s, 1H)	12.94 (s, 1H)			
12	11.90 (s, 1H)					
1'		5.67 (d, $J = 1.1$ Hz, 1H)	5.84 (s, 1H)		99.08	96.25
2'		4.01 (m, 1H),	3.71 (m, 1H),		70.54	80.65
3'		4.01 (m, 1H)	4.09 (m, 1H)		70.59	70.48
4'		3.35 (ddd, $J = 9.3$ Hz, 1H)	3.29 (m, 1H)		72.15	72.48
5'		3.51 (m, 1H)	3.51 (s, 1H)		70.66	70.46
6'- CH_3		1.10 (d, $J = 6.2$ Hz, 3H)	1.10 (d, $J = 6.3$ Hz, 3H)		18.35	18.33
12- $\text{O}-\text{CH}_3$			3.5 (s, 3H)			59.44

Coupling constant is represented as J , whereas multiplicities are indicated by s (singlet), d (doublet), and m (multiplet), and the chemical shift values are in ppm.

3.3. Anticancer Activities

The three compounds prepared were further analyzed for their in vitro cytotoxicities using 3-(4,5-dimethylthiazol-2-yl)-2,5-diphenyltetrazolium bromide (MTT) colorimetric assay against three different cancer cell lines (Figure 4) and one normal cell line (Figure S6). Two derivatives of chrysozin (i.e., CR and CRM) showed higher cytotoxicities than chrysozin. The 50% inhibitory concentration (IC_{50}) values of chrysozin for AGS, Huh7, and HL60 cells were 17.08, 30.53, and 22.24 (μM), respectively. Chrysozin-8- O - α -L-rhamnoside inhibited AGS, Huh7, and HL60 cells with 50% inhibitory concentration (IC_{50}) values of 28.58, 21.28, and 14.68 (μM), respectively. Here, CR showed better anticancer activities in Huh7 and HL60 than chrysozin. In the case of AGS cells, it showed slightly lower anticancer activity. In the case of chrysozin-8- O - α -L-2'- O -methylrhamnoside, it showed higher anticancer activities than chrysozin and CR. The 50% inhibitory concentration (IC_{50}) values of CRM for AGS, Huh7, and HL60 cells were 7.513, 4.467, and 4.540 (μM), respectively. In the case of the HaCaT normal cell line, the IC_{50} values were >200 μM for chrysozin, CR, and CRM (Table S1 and Figure S6). These compounds had a lower inhibitory

effect on normal cells. These results suggest that CR and CRM can remarkably reduce cell viabilities of AGS, Huh7, and HL60 cells in a dose-dependent manner. This is the first report of the activity of these two compounds against AGS, Huh7, and HL60 cells.

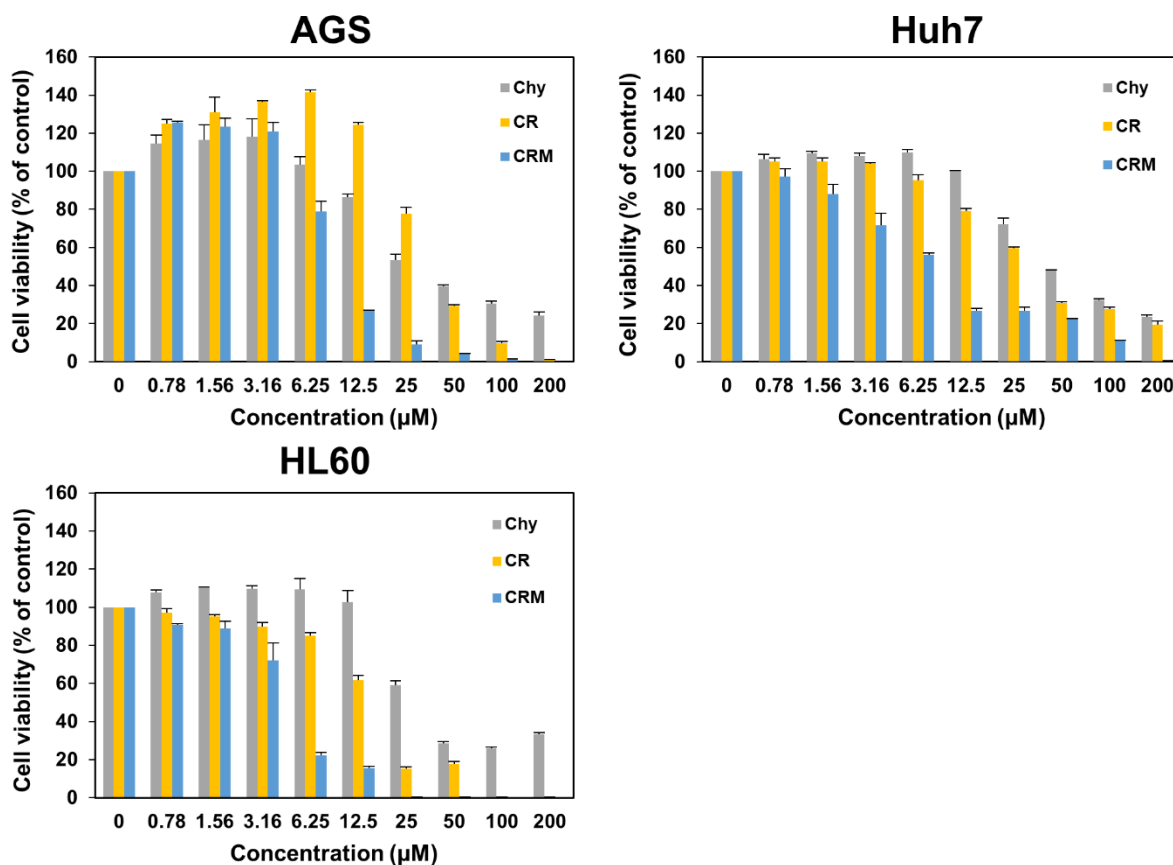


Figure 4. Cell cytotoxicity assay results of chrysazin, chrysazin-8-*O*- α -L-rhamnoside, and chrysazin-8-*O*- α -L-2'-*O*-methylrhamnoside. Cells were treated with various concentrations (0.0–200 μ M) of each compound.

3.4. Antimicrobial Bacterial Activities

3.4.1. Disk Diffusion Assay

Paper-disk diffusion assay was performed to determine the antimicrobial activity. All three compounds (chrysazin, CR, and CRM) were prepared at a concentration of 10 mg/mL. All compounds were added to each disk at a final concentration of 40 μ g/disk (4 μ L). Each disk was placed over Mueller–Hinton agar (MHA) plates spread with bacterial strains. The diameter of the zone of inhibition was measured after 18–20 h. Results of disk diffusion assays revealed that chrysazin did not show any antibacterial activity against 18 different human pathogens tested. However, CR and CRM exhibited antibacterial activities against Gram-positive bacteria *S. aureus* subsp. (Figure S5 and Table S2). These results reveal that rhamnosylation and rhamnose methylation of chrysazin might be profitable for heightening its antibacterial activity against different Gram-positive bacteria.

3.4.2. Measurement of MIC and MBC Values

Minimum inhibitory concentration (MIC) and minimum bactericidal concentration (MBC) for chrysazin, chrysazin-8-*O*- α -L-rhamnoside, and chrysazin-8-*O*- α -L-2'-*O*-methylrhamnoside against nine different pathogenic bacteria were determined. MIC values of compound chrysazin, CR, CRM, and erythromycin as a positive control, against nine strains of Gram-positive bacteria *S. aureus* subsp were determined by the broth dilution method. The assays were performed in 96-well plates in duplicate with Mueller–Hinton broth. As

summarized in Table 2, CR and CRM exhibited antibacterial activity against *S. aureus* CCARM 0205 (MSSA), *S. aureus* CCARM 0204 (MRSA), *S. aureus* CCARM 3640 (MRSA), *S. aureus* CCARM 3090 (MRSA), *S. aureus* CCARM 3634 (MRSA), *S. aureus* CCARM 0027 (MSSA), *S. aureus* CCARM 3089 (MRSA), *S. aureus* CCARM 3635 (MRSA), and *S. aureus* CCARM 33591(MRSA), with MIC values of 7.81–1000 µg/mL. After knowing the MIC value, we further analyzed MBC, the lowest concentration of a compound for killing inoculated bacteria. An MBC test was performed by inoculating cultured samples containing MIC compounds and experimental strains on a fresh MHB medium (Table 3). MBC values were similar to or higher than MIC values in all tested strains. Chrysazin did not show antibacterial activity against different pathogenic bacteria but derivatives of it, i.e., CR and CRM, improve its antibacterial activity. The metabolite showed significantly improved antibacterial activity against a wide range of Gram-positive MRSA and MSSA pathogens. Therefore, CR and CRM have great potential as an antibiotic against superbugs.

Table 2. MIC values of compound chrysazin, CR, CRM, and erythromycin (Erm) against 9 strains.

	MIC (µg/mL)			
	Chrysazin	CR	CRM	Erm
<i>S. aureus</i> CCARM 0205 (MSSA)	>1000	15.62	7.81	3.91
<i>S. aureus</i> CCARM 0204 (MRSA)	>1000	62.5	15.62	3.91
<i>S. aureus</i> CCARM 3640 (MRSA)	>1000	250	62.5	>1000
<i>S. aureus</i> CCARM 3090 (MRSA)	>1000	250	125	500
<i>S. aureus</i> CCARM 3634 (MRSA)	>1000	250	125	>1000
<i>S. aureus</i> CCARM 0027 (MSSA)	>1000	500	250	3.91
<i>S. aureus</i> CCARM 3089 (MRSA)	>1000	1000	500	>1000
<i>S. aureus</i> CCARM 3635 (MRSA)	>1000	1000	500	500
<i>S. aureus</i> CCARM 33591(MRSA)	>1000	>1000	500	>1000

Erm (erythromycin): positive control.

Table 3. MBC values of compound chrysazin, CR, CRM, and erythromycin (Erm) against 9 strains.

	MBC (µg/mL)			
	Chrysazin	CR	CRM	Erm
<i>S. aureus</i> CCARM 0205 (MSSA)	>1000	31.25	15.62	7.81
<i>S. aureus</i> CCARM 0204 (MRSA)	>1000	125	15.62	7.81
<i>S. aureus</i> CCARM 3640 (MRSA)	>1000	250	125	>1000
<i>S. aureus</i> CCARM 3090 (MRSA)	>1000	500	125	500
<i>S. aureus</i> CCARM 3634 (MRSA)	>1000	500	250	>1000
<i>S. aureus</i> CCARM 0027 (MSSA)	>1000	500	250	7.81
<i>S. aureus</i> CCARM 3089 (MRSA)	>1000	>1000	1000	>1000
<i>S. aureus</i> CCARM 3635 (MRSA)	>1000	1000	1000	1000
<i>S. aureus</i> CCARM 33591(MRSA)	>1000	>1000	1000	>1000

Erm (erythromycin): positive control.

4. Conclusions

In this study, we successfully engineered an *E. coli* strain for the sustainable production of different derivatives of chrysazin. Chrysazin-8-*O*- α -L-rhamnoside and chrysazin-8-*O*- α -L-2'-*O*-methylrhamnoside were novel compounds. We also evaluated their activities against three different cancer cell lines (AGS, Huh7, and HL60). CR and CRM exhibited higher cytotoxicities than their parental compound, chrysazin. More significantly, the evaluation of antibacterial activity revealed promising bioactivities of CR and CRM. This study establishes an engineered microbial platform that can be used to produce novel bioactive compounds. This microbial platform can be further fine-tuned for the production of novel derivatives of other anthraquinones or different compounds. Furthermore, the optimization of bioprocessing parameters and rational engineering of the host using various synthetic biological tools and metabolic engineering can be employed to enhance the production titer.

Supplementary Materials: The following supporting information can be downloaded at: <https://www.mdpi.com/article/10.3390/molecules27175554/s1>, Figure S1: Determination of optimum culture conditions using chrysazin as substrate. (A) The conversion rate of chrysazin using different substrate concentrations; the optimum concentration is 4 mM. (B) Conversion rate using different concentrations of glucose with the already determined substrate condition; the optimum glucose concentrations 10%. (C) Conversion rate of chrysazin in different time interval with the already determined conditions; the optimal time is 48 hrs. (Error bars show the standard deviation of three distinct experiments).; Figure S2: Different NMR spectrum of chrysazin; Figure S3: Different NMR spectrum of chrysazin-8-O- α -L-rhamnoside; Figure S4: Different NMR spectrum of chrysazin-8-O- α -L-2'-O-methylrhamnoside; Figure S5: Antibacterial activity of 1(DMSO), 2(Chrysazin), 3(CR), and 4(CRM) with (i) *S. aureus* CCARM 0204 (MSSA), (ii) *S. aureus* CCARM 0205 (MSSA), (iii) *S. aureus* CCARM 3090 (MRSA), (iv) *S. aureus* CCARM 3634 (MRSA), (v) *S. aureus* CCARM 3635 (MRSA), (vi) *S. aureus* CCARM 0027 (MSSA), (vii) *S. aureus* CCARM 3089 (MRSA), (viii) *S. aureus* CCARM 33591(MRSA) (ix) *S. aureus* CCARM 3640 (MRSA); Figure S6: Inhibitory effects of chrysazin, CR, and CRM on normal cell HaCaT growth; Table S1: Anticancer (IC₅₀ (μ M)) potential of chrysazin analogues against different cell lines.; Table S2: Antibacterial activities test against Gram-positive and Gram-negative bacteria via disc diffusion assay. The zone of inhibition (diameter) due to DMSO, chrysazin, chrysazin-8-O- α -L-rhamnoside, and chrysazin-8-O- α -L-2'-O-methylrhamnoside against different pathogens is noted in mm.

Author Contributions: P.B.P. performed the experiments and analyzed the data. D.D. designed and wrote the manuscript. R.T.M. performed other experiments. J.K.S. revised the manuscript and is supervision. All authors have read and agreed to the published version of the manuscript.

Funding: This work was supported by a grant from the Next-Generation BioGreen 21 Program (grant#: PJ01622901), Rural Development Administration, Korea.

Institutional Review Board Statement: Not applicable.

Informed Consent Statement: Not applicable.

Data Availability Statement: Not applicable.

Conflicts of Interest: The authors declare no conflict of interest.

References

1. Thomson, R.H. Anthraquinones. In *Naturally Occurring Quinones*; Elsevier: Amsterdam, The Netherlands, 1971; pp. 367–535. [[CrossRef](#)]
2. Yen, G.C.; Der Duh, P.; Chuang, D.Y. Antioxidant Activity of Anthraquinones and Anthrone. *Food Chem.* **2000**, *70*, 437–441. [[CrossRef](#)]
3. Agarwal, S.K.; Singh, S.S.; Verma, S.; Kumar, S. Antifungal Activity of Anthraquinone Derivatives from Rheum Emodi. *J. Ethnopharmacol.* **2000**, *72*, 43–46. [[CrossRef](#)]
4. Barnard, D.L.; Huffman, J.H.; Morris, J.L.B.; Wood, S.G.; Hughes, B.G.; Sidwell, R.W. Evaluation of the Antiviral Activity of Anthraquinones, Anthrones and Anthraquinone Derivatives against Human Cytomegalovirus. *Antivir. Res.* **1992**, *17*, 63–77. [[CrossRef](#)]
5. Choi, S.Z.; Lee, S.O.; Jang, K.U.; Chung, S.H.; Park, S.H.; Kang, H.C.; Yang, E.Y.; Cho, H.J.; Lee, K.R. Antidiabetic Stilbene and Anthraquinone Derivatives from Rheum Undulatum. *Arch. Pharm. Res.* **2005**, *28*, 1027–1030. [[CrossRef](#)]
6. Kshirsagar, A.D.; Panchal, P.V.; Harle, U.N.; Nanda, R.K.; Shaikh, H.M. Anti-Inflammatory and Antiarthritic Activity of Anthraquinone Derivatives in Rodents. *Int. J. Inflamm.* **2014**, *2014*, 1–12. [[CrossRef](#)]
7. Schörkhuber, M.; Richter, M.; Dutter, A.; Sontag, G.; Marian, B. Effect of Anthraquinone-Laxatives on the Proliferation and Urokinase Secretion of Normal, Premalignant and Malignant Colonic Epithelial Cells. *Eur. J. Cancer* **1998**, *34*, 1091–1098. [[CrossRef](#)]
8. Duval, J.; Pecher, V.; Poujol, M.; Lesellier, E. Research Advances for the Extraction, Analysis and Uses of Anthraquinones: A Review. *Ind. Crop. Prod.* **2016**, *94*, 812–833. [[CrossRef](#)]
9. Koyama, J.; Morita, I.; Tagahara, K.; Nobukuni, Y.; Mukainaka, T.; Kuchide, M.; Tokuda, H.; Nishino, H. Chemopreventive Effects of Emodin and Cassiamin B in Mouse Skin Carcinogenesis. *Cancer Lett.* **2002**, *182*, 135–139. [[CrossRef](#)]
10. Akev, N.; Candoken, E.; Kuruca, S.E. Comparative Study on the Anticancer Drug Potential of a Lectin Purified from Aloe Vera and Aloe-Emodin. *Asian Pac. J. Cancer Prev.* **2020**, *21*, 99–106. [[CrossRef](#)]
11. Huang, Q.; Lu, G.; Shen, H.M.; Chung, M.C.M.; Choon, N.O. Anticancer Properties of Anthraquinones from Rhubarb. *Med. Res. Rev.* **2007**, *27*, 609–630. [[CrossRef](#)]

12. Al-Otaibi, J.S.; EL Gogary, T.M. Synthesis of Novel Anthraquinones: Molecular Structure, Molecular Chemical Reactivity Descriptors and Interactions with DNA as Antibiotic and Anticancer Drugs. *J. Mol. Struct.* **2017**, *1130*, 799–809. [[CrossRef](#)]
13. Madje, B.R.; Shelke, K.F.; Sapkal, S.B.; Kakade, G.K.; Shingare, M.S. An Efficient One-Pot Synthesis of Anthraquinone Derivatives Catalyzed by Alum in Aqueous Media. *Green Chem. Lett. Rev.* **2010**, *3*, 269–273. [[CrossRef](#)]
14. Seidel, N.; Hahn, T.; Liebing, S.; Seichter, W.; Kortus, J.; Weber, E. Synthesis and Properties of New 9,10-Anthraquinone Derived Compounds for Molecular Electronics. *New J. Chem.* **2013**, *37*, 601–610. [[CrossRef](#)]
15. Le, T.T.; Pandey, R.P.; Gurung, R.B.; Dhakal, D.; Sohng, J.K. Efficient enzymatic systems for synthesis of novel α -mangostin glycosides exhibiting antibacterial activity against Gram-positive bacteria. *Appl. Microbiol. Biotechnol.* **2014**, *98*, 8527–8538. [[CrossRef](#)] [[PubMed](#)]
16. Nguyen, T.T.H.; Pandey, R.P.; Parajuli, P.; Han, J.M.; Jung, H.J.; Park, Y.; Sohng, J.K. Microbial Synthesis of Non-Natural Anthraquinone Glucosides Displaying Superior Antiproliferative Properties. *Molecules* **2018**, *23*, 2171. [[CrossRef](#)]
17. Koirala, N.; Huy, N.; Prasad, G.; Van Thang, D.; Sohng, J.K. Enzyme and Microbial Technology Methylation of Flavonoids: Chemical Structures, Bioactivities, Progress and Perspectives for Biotechnological Production. *Enzym. Microb. Technol.* **2016**, *86*, 103–116. [[CrossRef](#)]
18. Kctc, S.; Kim, T.; Kyung, J. Enzyme and Microbial Technology Characterization of Regioselective Fl Avonoid O- Methyltransferase from *Streptomyces* sp. KCTC 0041BP. *Enzym. Microb. Technol.* **2018**, *113*, 29–36. [[CrossRef](#)]
19. Michalak, E.M.; Burr, M.L.; Bannister, A.J.; Dawson, M.A. The Roles of DNA, RNA and Histone Methylation in Ageing and Cancer. *Nat. Rev. Mol. Cell Biol.* **2019**, *20*, 573–589. [[CrossRef](#)]
20. Staudacher, E. Methylation—an Uncommon Modification of Glycans. *Biol. Chem.* **2012**, *393*, 675–685. [[CrossRef](#)]
21. Ripoll-Rozada, J.; Costa, M.; Manso, J.A.; Maranhã, A.; Miranda, V.; Sequeira, A.; Rita Ventura, M.; Macedo-Ribeiro, S.; Pereira, P.J.B.; Empadinhas, N. Biosynthesis of Mycobacterial Methylmannose Polysaccharides Requires a Unique 1-O-Methyltransferase Specific for 3-O-Methylated Mannosides. *Proc. Natl. Acad. Sci. USA* **2019**, *116*, 835–844. [[CrossRef](#)]
22. Gutmann, A.; Schiller, M.; Gruber-Khadjawi, M.; Nidetzky, B. An: Ortho C -Methylation/O -Glycosylation Motif on a Hydroxy-Coumarin Scaffold, Selectively Installed by Biocatalysis. *Org. Biomol. Chem.* **2017**, *15*, 7917–7924. [[CrossRef](#)] [[PubMed](#)]
23. Xie, L.; Zhang, L.; Bai, J.; Yue, Q.; Zhang, M.; Li, J.; Wang, C.; Xu, Y. Methylglucosylation of Phenolic Compounds by Fungal Glycosyltransferase-Methyltransferase Functional Modules. *J. Agric. Food Chem.* **2019**, *67*, 8573–8580. [[CrossRef](#)] [[PubMed](#)]
24. Chiang, J.-H.; Yang, J.-S.; Ma, C.-Y.; Yang, M.-D.; Huang, H.-Y.; Hsia, T.-C.; Kuo, H.-M.; Wu, P.-P.; Lee, T.-H.; Chung, J.-G. Danthron, an Anthraquinone Derivative, Induces DNA Damage and Caspase Cascades-Mediated Apoptosis in SNU-1 Human Gastric Cancer Cells through Mitochondrial Permeability Transition Pores and Bax-Triggered Pathways. *Chem. Res. Toxicol.* **2010**, *24*, 20–29. [[CrossRef](#)]
25. Chiou, S.M.; Chiu, C.H.; Yang, S.T.; Yang, J.S.; Huang, H.Y.; Kuo, C.L.; Chen, P.Y.; Chung, J.G. Danthron Triggers ROS and Mitochondria-Mediated Apoptotic Death in C6 Rat Glioma Cells through Caspase Cascades, Apoptosis-Inducing Factor and Endonuclease G Multiple Signaling. *Neurochem. Res.* **2012**, *37*, 1790–1800. [[CrossRef](#)]
26. Strobe, T.; Schmidt, Y.; Linnenbrink, A.; Luzhetskyy, A.; Luzhetskya, M.; Taguchi, T.; Brötz, E.; Paululat, T.; Stasevych, M.; Stanko, O.; et al. Tracking down Biotransformation to the Genetic Level: Identification of a Highly Flexible Glycosyltransferase from *Saccharothrix Espanaensis*. *Appl. Environ. Microbiol.* **2013**, *79*, 5224–5232. [[CrossRef](#)]
27. Mishra, R.; Dhakal, D.; Han, J.M.; Lim, H.N.; Jung, H.J.; Yamaguchi, T.; Sohng, J.K. Production of a Novel Tetrahydroxynaphthalene (THN) Derivative from *Nocardia* Sp. CS682 by Metabolic Engineering and Its Bioactivities. *Molecules* **2019**, *24*, 244. [[CrossRef](#)]
28. Choi, H.R.; Park, J.S.; Kim, K.M.; Kim, M.S.; Ko, K.W.; Hyun, C.G.; Ahn, J.W.; Seo, J.H.; Kim, S.Y. Enhancing the Antimicrobial Effect of Genistein by Biotransformation in Microbial System. *J. Ind. Eng. Chem.* **2018**, *63*, 255–261. [[CrossRef](#)]
29. Thi, T.; Nguyen, H.; Shin, H.J.; Pandey, R.P.; Jung, H.J.; Liou, K.; Sohng, J.K. Biosynthesis of Rhamnosylated Anthraquinones in *Escherichia Coli*. *J. Microbiol. Biotechnol.* **2020**, *30*, 398–403. [[CrossRef](#)]
30. Poudel, P.B.; Pandey, R.P.; Dhakal, D.; Kim, T.-S.; Thi, T.; Nguyen, H.; Jung, H.J.; Shin, H.J.; Timalisina, B.; Sohng, J.K. Functional Characterization of a Regiospecific Sugar-O-Methyltransferase from *Nocardia*. *Appl. Environ. Microbiol.* **2022**, *88*, 1–11. [[CrossRef](#)]
31. Parajuli, P.; Pandey, R.P.; Trang, N.T.H.; Chaudhary, A.K.; Sohng, J.K. Synthetic Sugar Cassettes for the Efficient Production of Flavonol Glycosides in *Escherichia Coli*. *Microb. Cell Fact.* **2015**, *14*, 1–12. [[CrossRef](#)]
32. M02-A11; Performance Standards for Antimicrobial Disk Susceptibility Tests. Clinical and Laboratory Standards Institute: Malvern, PA, USA, 2012.
33. Hudzicki, J. Kirby-Bauer Disk Diffusion Susceptibility Test Protocol Author. *Am. Soc. Microbiol.* **2009**, 1–13. Available online: <https://www.asm.org/Protocols/Kirby-Bauer-Disk-Diffusion-Susceptibility-Test-Pro> (accessed on 22 July 2020).
34. Wiegand, I.; Hilpert, K.; Hancock, R.E.W. Agar, and Broth Dilution Methods to Determine the Minimal Inhibitory Concentration (MIC) of Antimicrobial Substances. *Nat. Protoc.* **2008**, *3*, 163–175. [[CrossRef](#)] [[PubMed](#)]